Ultrastable CO_2 Lasers

C. Freed

This article begins with a brief review of gas-laser research and the events that led to the development of ultrastable CO_2 lasers at Lincoln Laboratory. Extremely high spectral purity and short-term stabilities of $\Delta f/f < 1.5 \times 10^{-13}$ have been routinely achieved with these ultrastable CO_2 lasers. At MIT/Lincoln Laboratory, we have also invented a novel frequency stabilization method that enabled the long-term frequency locking of CO_2 (and many other) molecular lasers to the center frequency of any regular- or hot-band CO_2-isotope-laser transition. Consequently, line-center-stabilized CO_2-isotope lasers have become the best secondary frequency standards known to date in the infrared domain. Some of the output characteristics, selected applications, and design features of the lasers are also described. The article concludes with a discussion of some of the advantages and limitations of the present laser design.

Carbon-dioxide lasers were invented by C.K.N. Patel in 1964 [1], and by mid-1965 he had demonstrated CW output powers that exceeded 10 W [2]. It was the first time that any single laser had achieved a CW or average-power level exceeding 1 W. Thus the CO_2 laser became the first, and 25 years later it remains the best, laser for long-range Doppler and imaging optical radars [3–5]. The recent successes of the Firefly tests carried out with the CO_2-laser radar facility at the Lincoln Laboratory Firepond site in Westford, Mass., in March [6] and October 1990 have amply supported the above statement.

The development of ultrastable CO_2 lasers was a direct outgrowth of previous work and experience with stable He-Ne lasers at MIT/Lincoln Laboratory. Research on gas lasers started at Lincoln Laboratory around the beginning of 1963. At the time, most gas lasers were based on the He-Ne system that A. Javan had invented in 1960 [7]. By early 1963, C.H. Townes, Javan, and coworkers had clearly established the inherently good spectral purity and short-term frequency stability of He-Ne lasers [8] in a series of experiments to test special relativity [9]. These experiments, the famous "ether drift" measurements carried out in the wine cellar of the Round Hill Estate of MIT [8], utilized pairs of very stable He-Ne lasers, the design of which was developed by Javan and his colleagues. Javan's design called for a very rigid optical cavity that consisted of four 1-inch-diameter invar rod spacers and two internal mirrors (i.e., mirrors within the vacuum envelope that contained the laser gas mixture).

The first stable gas laser that we designed and constructed at Lincoln Laboratory departed from Javan's design only in minor details; for example, the laser was made with demountable metallic (conflat) vacuum seals instead of brazed joints. The features that contributed to laser stability, i.e., the rigid invar rod cavity and the internal mirrors, were essentially retained intact. Two such He-Ne lasers were built and extensively utilized to study the intensity fluctuations of laser output just below and above the oscillation threshold.

It should be noted that during the early period of laser history (1960 to 1963) there was a great deal of interest and outright controversy about the nature and appropriate analytical description of the light emitted by lasers [10]. C.H. Townes suggested to H.A. Haus and me that this topic would be very suitable for us to investigate. Our subsequent research and publications [11–16] on the photocurrent spectrum and photoelectron counts produced by a He-Ne gas laser have clearly shown that the spontaneous emission in the vicinity of lasing threshold can dominate the amplitude noise of a laser. However, it did require a great deal of learning and the development of refined experimental techniques to operate the lasers with sufficient stability in the vicinity of the oscillating threshold. Consequently, satisfying the requirement for stable CO_2 lasers at Lincoln Laboratory three years later (1966) was straightforward: the conver-

sion from He-Ne to CO_2 operation was simply a matter of changing two mirrors and an output window, and providing a water-cooled discharge tube and a CO_2 laser gas mixture. Even our initial measurements with the first pair of these lasers converted from He-Ne to CO_2 operation demonstrated stabilities at least 100 times better than previously reported [17], and the demand at Lincoln Laboratory for additional CO_2 lasers skyrocketed virtually overnight.

Thus we undertook a complete redesign of the stable laser structure at that time, and within about a year (by early 1968) we had the first batch of the redesigned ultrastable CO_2 lasers in operation [18]. (Today, more than 20 years later, dozens of these ultrastable lasers are still in operation at Lincoln Laboratory.) In 1970 we also demonstrated the first completely sealed-off and ultrastable operation of the molecular CO laser system by using these redesigned CO_2 lasers [19, 20].

Within Lincoln Laboratory the ultrastable CO_2/CO lasers were, and still are, primarily used in optical radars, heterodyne spectroscopy, and optical pumping, and for the study of various processes in laser physics and kinetics by MIT/Lincoln Laboratory staff and graduate students.

Many additional ultrastable lasers were built elsewhere from the detailed design drawings that Lincoln Laboratory furnished to qualified researchers at various universities and laboratories in the United States and Great Britain. A complete listing of the various users and applications is obviously well beyond the scope of this paper; I will briefly mention the two that I personally found most gratifying and rewarding. The first is the use of ultrastable CO_2 lasers for infrared heterodyne spectroscopy in planetary (Mars and Venus) atmospheres by C.H. Townes and his collaborators at the University of California, Berkeley [21, 22]. The second is the high-altitude balloon-borne experiment that used a sealed-off CO laser pump with which C.K.N. Patel first demonstrated the depletion of high-altitude ozone by the complex interaction of sunlight and chlorofluorocarbon compounds.

The main body of this article has four sections:

1. spectral purity and short-term stability,
2. long-term, line-center stabilization of CO_2 lasers,
3. CO_2-isotope lasers as secondary frequency standards, and
4. laser design.

At this time I would like to point out that this article is only a brief review of more than 25 years of work. Also, the results reported here represent the cumulative efforts of many individuals in the MIT/Lincoln Laboratory community. The acknowledgments at the end list those who most significantly contributed to this endeavor.

Spectral Purity and Short-Term Stability

The theoretical linewidth of a laser above threshold was first derived by Schawlow and Townes and published in 1958 [23], about two years before the actual demonstration of the first laser, which was made from ruby, by T.H. Maiman in 1960 [24]. In its simplest form the Schawlow-Townes theory predicted that the output power P_o of a laser will have a Lorentzian line shape with a quantum-noise-limited full width at half maximum (FWHM) Δf approximated by

$$\Delta f \approx \frac{a\pi h f_0}{P_o}\left(\frac{f_0}{Q_c}\right)^2,$$

where a, h, f_0, P_o, and Q_c denote the population-inversion parameter, Planck's constant, the center frequency, the output power, and the cold-cavity Q of the laser (i.e., the Q of the cavity without any active medium), respectively.

In a well-designed CO_2 laser, Q_c is given by

$$Q_c \approx \frac{2\pi L f_0}{c T_r}, \qquad (1)$$

where L, c, and T_r denote the cavity length, speed of light in vacuum, and mirror transmission, respectively. (Diffraction losses are not included in Equation 1 because they are usually negligible compared to the output coupling loss). For a small CO_2 laser with $L = 50$ cm and $T_r = 5\%$, Q_c is on the order of 10^7. Thus for a typical power output of 1 to 10 W (which a small TEM_{00q}-mode CO_2 laser can easily supply) the quantum-phase-noise-limited linewidth is less than 10^{-6} Hz. Note that 10^{-6} Hz represents less than 1 part in 10^{19} of the output frequency ($f_0 \sim 3 \times 10^{13}$ Hz) of a CO_2 laser. This inherent spectral purity of CO_2 lasers can be explained as follows: the linewidth Δf is inversely proportional to the product of P_o and Q_c^2, and the combination of high P_o and high Q_c can be simultaneously achieved with relative ease even in a small CO_2-laser oscillator. Oscillators in the radio-frequency (RF) and microwave do-

main have either high P_o or high Q_c but not both together in a single device.

Laser stabilities are most frequently determined in the laboratory from the results of heterodyne experiments with two lasers. In a typical heterodyne experiment the output beams of the two lasers are combined by a beam splitter. The colinearly propagating wavefront of the two lasers is intercepted by a photon detector whose output current $i(t)$ will contain (in addition to dc currents) a component $i(t)_{IF}$ at the difference frequency

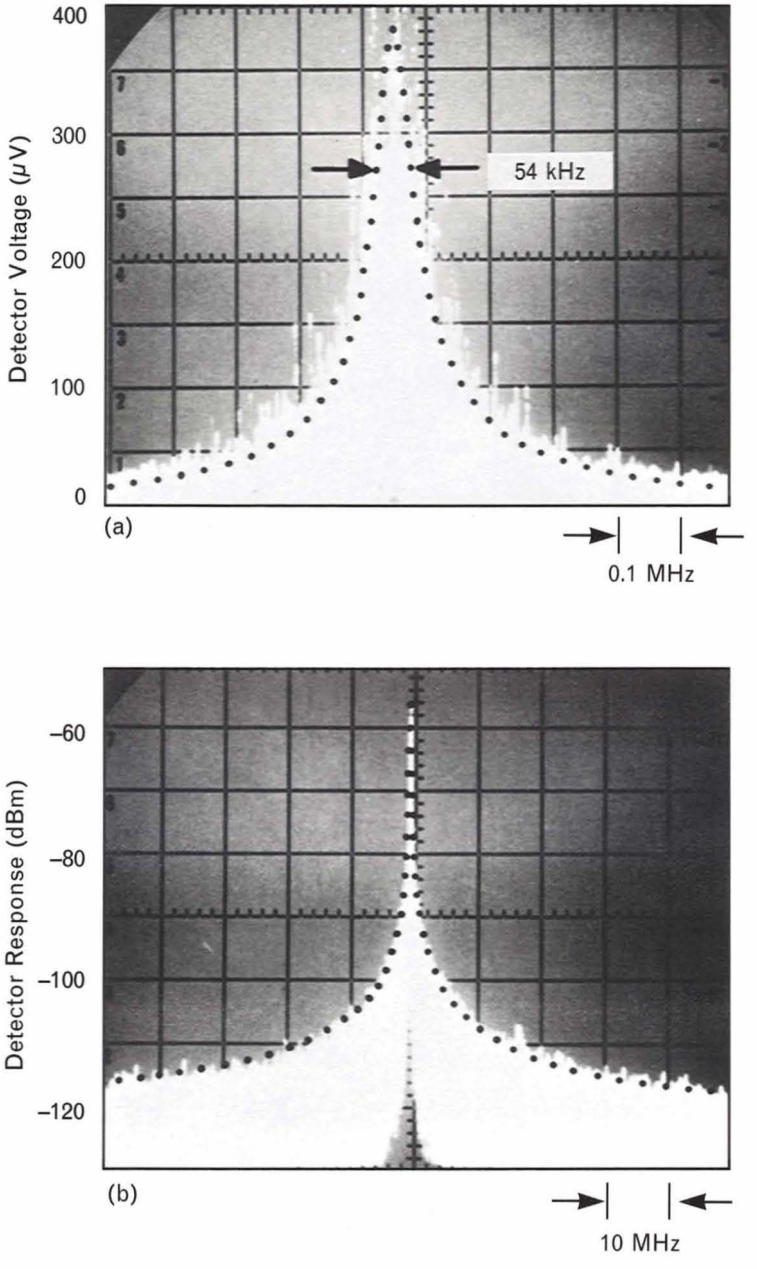

FIGURE 1. Spectrum-analyzer display of beat note between a 240-μW single-frequency $Pb_{0.88}Sn_{0.12}Te$ diode laser (well above threshold) and the P(14) transition of the CO_2 gas laser. The intermediate-frequency (IF) bandwidth is 10 kHz and the sweep rates and exposure times are (a) 0.2 sec/division and 2 sec, and (b) 0.002 sec/division and 0.5 sec, respectively. The dotted curves correspond to 54-kHz-bandwidth Lorentzian fits to the power spectral density. Note that the photo in *b* contains ~25 consecutively recorded superimposed traces.

(also called the beat frequency, or intermediate frequency) of the two lasers:

$$i(t)_{IF} = 2\sqrt{i_{lo}i_s}\cos(\omega_{lo} - \omega_s)t.$$

In order to differentiate between the two individual laser outputs, the subscripts lo and s are used to denote the local-oscillator and signal-oscillator parameters, respectively.

Laser stabilities can be determined by either frequency-domain (Fourier spectrum) or time-domain (Allan variance) analysis of the beat-note spectra of the laser pairs. If the spectral purity of one of the lasers (typically the local oscillator) is much better than that of the other laser, then the beat-note spectrum may be entirely attributed to the worse of the two lasers. For example, even for a high-quality lead-salt solitary diode laser the power output is only on the order of a milliwatt and Q_c is less than 10. Thus the quantum-phase-noise-limited Schawlow-Townes linewidth prediction is typically in the tens of kilohertz, in contrast with the 10^{-6} Hz predicted for a CO_2 laser. We took advantage of these characteristics of the CO_2 and lead-salt diode lasers in the historic first experimental demonstration and verification of the Lorentzian line shape and FWHM linewidth of Schawlow and Townes [25] (Figure 1).

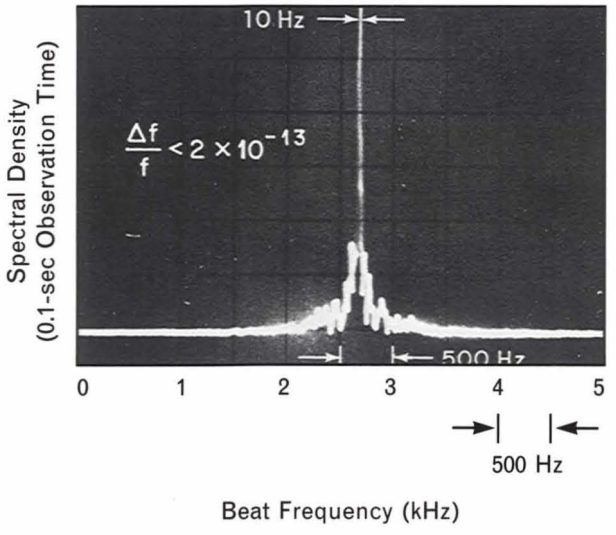

FIGURE 2. Real-time power spectrum of the beat signal between two free-running CO_2 lasers. The horizontal scale of the figure is 500 Hz/division, which indicates that the optical frequencies of the two lasers producing the beat note were offset by less than 3 kHz. The 10-Hz width of the line shown is limited by instrumentation; the linewidth of the beat note falls within this limit.

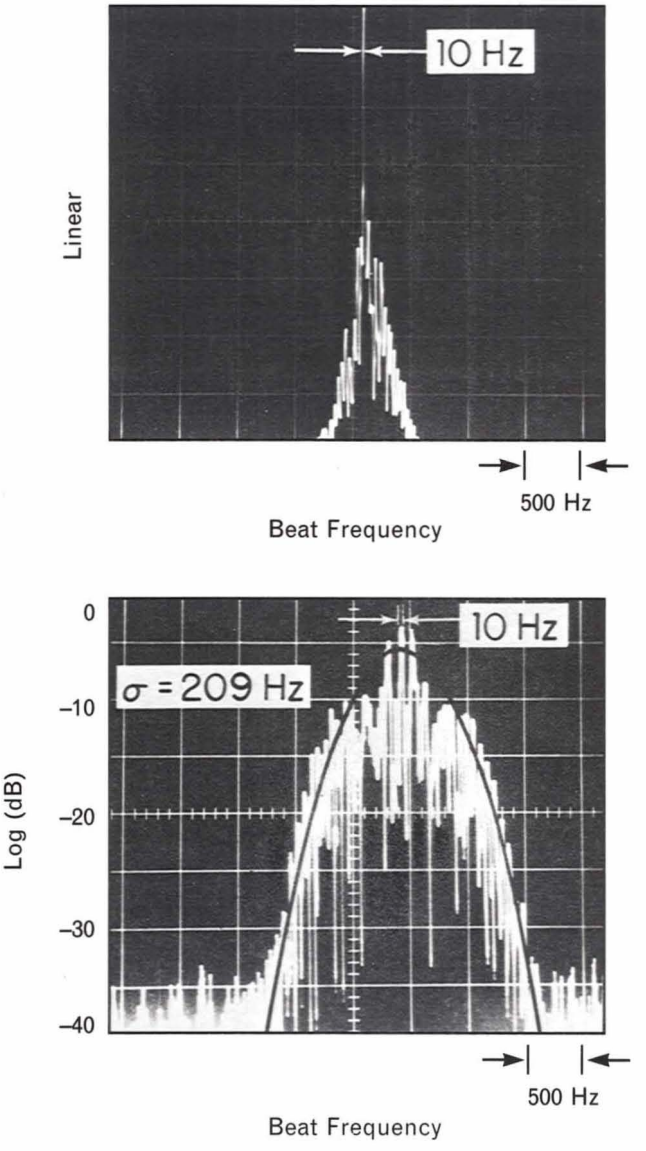

FIGURE 3. Same as Figure 2, but with increased acoustical background noise coupled to the lasers. Note that the spectral lines have a Gaussian-line-shape envelope.

To establish the spectral purity of the CO_2 laser itself, we can heterodyne two CO_2 lasers of equal high quality so that the resulting beat-note spectrum can be apportioned equally to each laser. Two problems arise, however, in trying to measure the Schawlow-Townes linewidth of high-quality CO_2 lasers. The first of these problems is instrumental: the stability of the available instrumentation is generally insufficient for reliable measurements of spectral purities of 10^{-6} Hz or better.

The origin of the second problem is that for well-

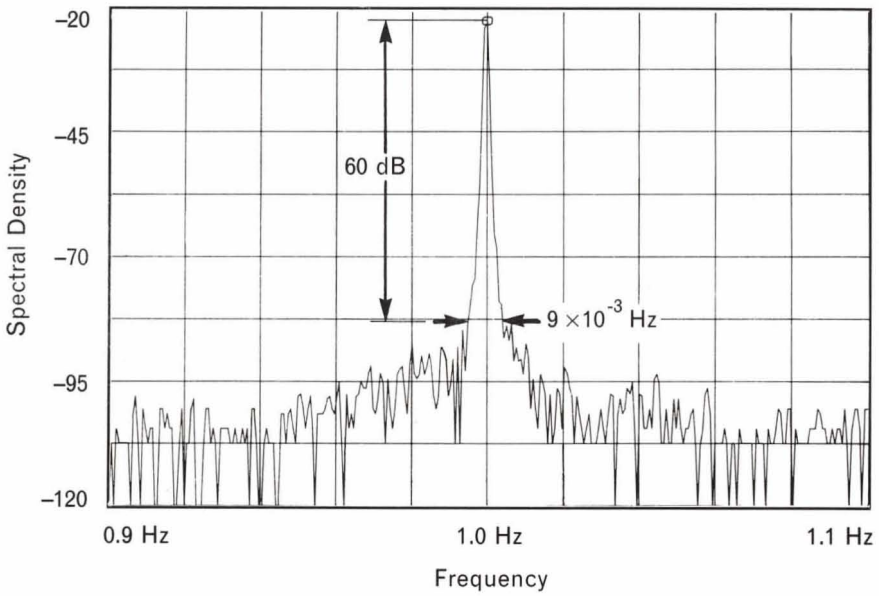

FIGURE 4. Spectral purity of beat note between two CO_2 lasers that were phase locked to each other with a frequency offset of 10 MHz. The FWHM spectral width of the beat note was about 9×10^{-6} Hz during the 26.67-min measurement time.

designed CO_2 lasers the so-called technical noise sources dominate over the quantum-phase-noise-limited Schawlow-Townes linewidth [26]. Examples of technical noise sources are acoustic and seismic vibrations, and power-supply ripple and noise. These sources can cause frequency instabilities by perturbing the effective cavity resonance via the sum of fractional changes in the refractive index n and the optical-cavity length L:

$$\Delta f = f\left(\frac{\Delta n}{n} + \frac{\Delta L}{L}\right).$$

As an example, a change of only 10^{-3} Å (about 1/1000 of the diameter of a hydrogen atom) in a 50-cm-long CO_2-laser cavity will cause a frequency shift of approximately 6 Hz. A 6-Hz variation in the approximately 3×10^{13}-Hz frequency of a CO_2 laser corresponds to a fractional instability of 2×10^{-13}. Figure 2, which shows the real-time power spectrum of the beat signal between two free-running lasers that we designed and built at Lincoln Laboratory [18], implies a frequency stability at least as good as 2×10^{-13}. The discrete modulation sidebands in the figure were primarily due to ac-power-line frequency harmonics, cooling-fan noise, and slow frequency drift; however, each spectral line was generally within the 10-Hz resolution bandwidth of the spectrum analyzer. The measurement of the spectral width was limited to a 10-Hz resolution by the 0.1-sec observation time that was set by the instrumentation, not by the laser stability itself.

Figure 3 shows another beat note of the same two lasers as in Figure 2, but with increased acoustical background noise coupled to the lasers [27]. The increased level of the spurious modulation sidebands that resulted from the noise is self-evident in the figure. The logarithmic display of Figure 3 also shows that the spectral lines fit within the Gaussian-line-shape envelope given by the expression

$$\frac{1}{\sigma\sqrt{2\pi}} \exp -\left[\frac{(f - f_0)^2}{2\sigma^2}\right]$$

with $\sigma = 209$ Hz fitted to the beat-note spectrum. Also note that the levels of the spurious modulation spectral lines fall at least 35 dB below the beat note's carrier frequency for frequencies that are spaced more than 1.2 kHz from the carrier frequency.

The spectra shown in Figures 2 and 3 clearly imply that by frequency- and/or phase-locking two stable CO_2 lasers with feedback-loop bandwidths of only a few kilohertz, we can overcome the masking effects of the spurious modulation sidebands.

Figure 4 shows the real-time power spectrum of the beat note of two ultrastable CO_2 lasers that were phase

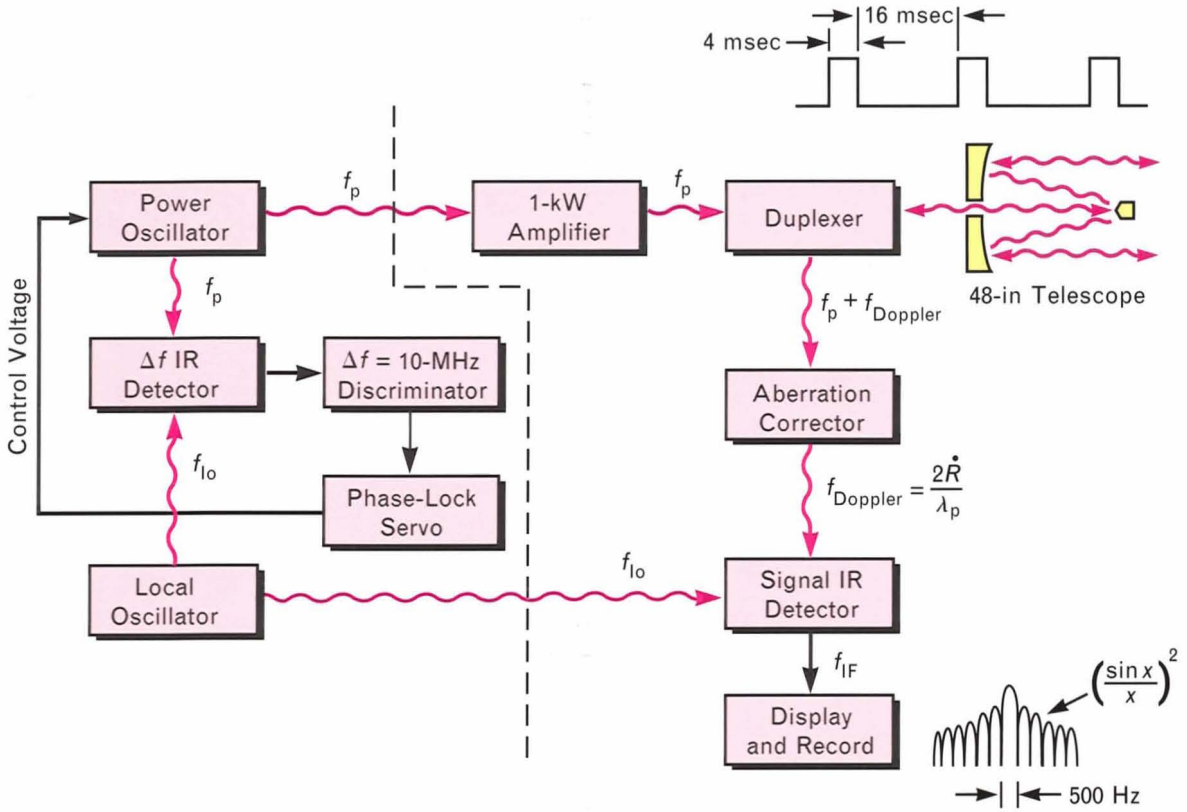

FIGURE 5. Simplified block diagram of a narrowband configuration of the CO_2 laser radar at the Lincoln Laboratory Firepond Facility in Westford, Mass. In the figure, wavy and solid lines denote optical and electrical signal paths, respectively.

locked with a fixed 10-MHz frequency offset between the two lasers and with the unity-gain bandwidth of the servoamplifier set to about 1.2 kHz [28]. Note that the horizontal scale in the figure is only 2×10^{-2} Hz/division and the vertical scale is logarithmic, with 12.5 dB/division. Using the results from Figure 4 and the equation for a Lorentzian line shape, we calculate the FWHM spectral width of the beat note to be about 9×10^{-6} Hz.

It took 26.67 min of measurement time to obtain just a single scan with the frequency resolution of Figure 4. Because tracking even by a very good servosystem would still be limited by quantum phase noise, the narrow linewidth in Figure 4 is an indirect but clear confirmation of the high spectral purity of CO_2 lasers, as predicted by the Schawlow-Townes formula.

Laser stabilities are most conveniently evaluated from the beat-note spectra of two lasers, as shown in Figures 2, 3, and 4. However, the results are not altogether foolproof because the disturbances that cause frequency jitter can be at least partially correlated. In an optical radar we can compare a laser with its own output delayed by the round-trip time to and from the target. Hence, effects due to disturbances with correlation times less than the round-trip time of the transmitted signal will be included in the measured beat-note spectrum.

Figure 5 shows a greatly simplified block diagram of a narrowband configuration of the CO_2-laser radar at the Lincoln Laboratory Firepond Facility. The 0.5-m-long local oscillator and the 1.5-m-long power oscillator were designed and constructed at Lincoln Laboratory. The higher power oscillator was phase locked to the local oscillator with a fixed 10-MHz frequency offset between the two lasers. Figure 4 has shown the beat-note spectrum of these two lasers.

The frequency stability of the CO_2-laser-radar facility at Firepond was verified from observations on GEOS-III, a NASA geodetic satellite that is equipped with an IRTRAN II solid-cube-corner retroreflector. Doppler measurements of the radar returns from GEOS-III helped to determine the radial velocity of the satellite, and to set an upper bound to the laser-oscillator instability [29]. During the measurements the satellite

range was 1063 km, which corresponded to a round-trip signal travel time of ~7 msec. In this particular radar experiment a duplexer chopped the constant-frequency amplified CO_2-laser-output signal so that a 25%-duty-cycle pulse train consisting of 4-msec-duration pulses spaced 16 msec apart was transmitted to the orbiting satellite.

Figure 6 shows the spectra that resulted from an RF test signal of 4-msec duration processed in the same manner as the optical radar data [28, 29]. In the figure, the horizontal rows simulate logarithmic displays of the power spectra of a consecutive sequence of radar return signals. The $[(\sin x)/x]^2$ spectral envelope, which is due to the 4-msec pulse duration, is quite evident. The average spectral width 10 dB below the peak is 383 Hz, and the standard deviation of the spectral width is 5 Hz.

Figure 7 shows the actual CO_2-radar return signal from GEOS-III at a 1063-km range [28, 29]. Notice the striking similarity to the simulated signal return of Figure 6, which was obtained from a high-quality frequency synthesizer that was also part of the radar receiver. A comparison of Figures 6 and 7 shows that the –10-dB average spectral width of the radar return signal broadened from 383 to 399 Hz and the standard deviation of this spectral width increased from 5 to 18.5 Hz. According to these figures, the short-term stability of the entire CO_2 radar system, including

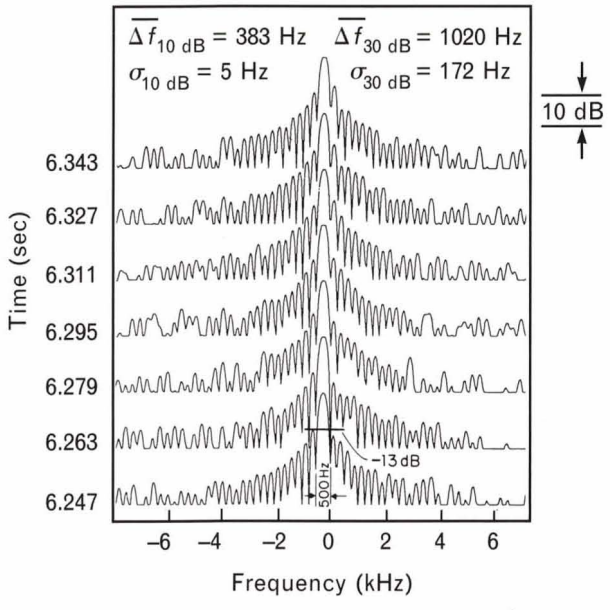

FIGURE 6. Simulated radar returns for a 4-msec-duration RF test signal.

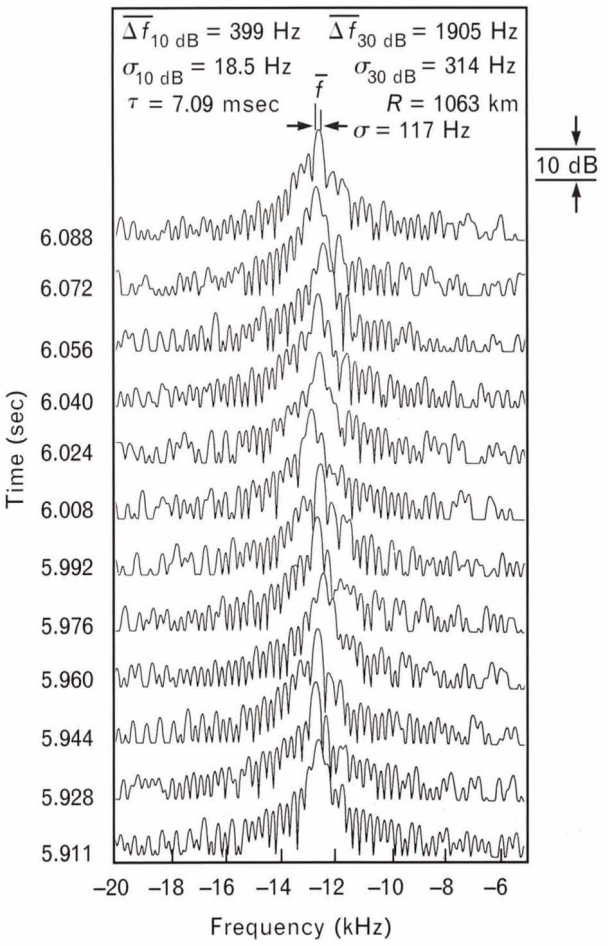

FIGURE 7. A consecutive sequence of actual radar return signals from GEOS-III.

round-trip propagation effects caused by fluctuations in the atmosphere, was better than 1.5×10^{-13} for the 7-msec round-trip duration.

Figure 7 also shows that the standard deviation of pulse-to-pulse centroid jitter of the spectra was 117 Hz during the test run. No effort was made to line-center-stabilize either of the lasers because the long-term stability of the free-running laser was more than adequate for typical optical radar applications.

Long-Term Line-Center Stabilization of CO_2 Lasers

Lasers can possess exceptionally high spectral purity and short-term frequency stability. Long-term stability, however, is generally lacking because all lasers are more or less tunable over a frequency band that is determined by the detailed physics of the gain-profile characteristics of each particular laser system.

In a typical low-pressure (~15 Torr) CO_2 laser, the

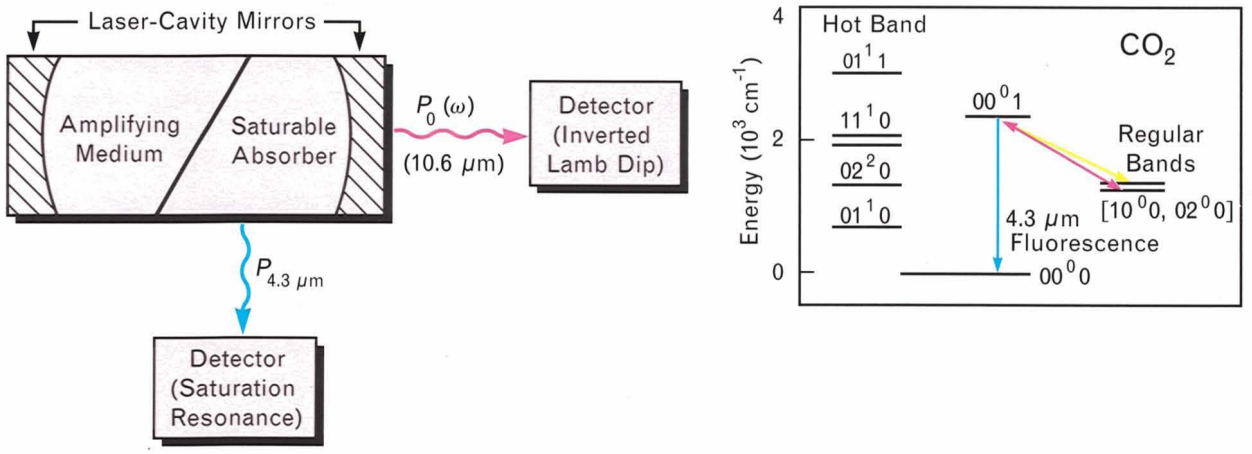

FIGURE 8. Graphic illustration of the saturation resonance observed in CO_2 fluorescence at 4.3 μm. Resonant interaction occurs for $\omega = \omega_0$ (when $\mathbf{k} \cdot \mathbf{v} = 0$). The figure shows an internal absorption cell within the laser cavity. External cells can also be used.

width of the gain profile is about 53 MHz and is dominated by Doppler broadening. In a high-pressure (~760 Torr) CO_2 laser, the width of the gain profile is dominated by pressure broadening, which is approximately 4 GHz/760 Torr for typical CO_2-laser gas mixtures. Thus even the ultrastable low-pressure (~15 Torr) CO_2 lasers are tunable: they may operate anywhere up to at least tens of MHz away from the center frequency of the oscillating transition and will generally drift back and forth due to changes in power-supply current and ambient temperature.

In many applications such as high-precision spectroscopy and multistatic radar it is highly desirable to find a narrow and frequency-stable reference (absorption) line within the operating range of the laser so that the laser can be frequency-locked or frequency-offset-locked to the reference line. Initial attempts to use CO_2 itself as a reference via either the Lamb-dip or the inverted-Lamb-dip techniques were not very successful. The poor results were obtained because the lower-state rotational-vibrational levels of the CO_2 laser transitions do not belong to the ground state, and therefore the absorption coefficient of low-pressure room-temperature CO_2 at 10 μm is very low. The low absorption coefficient in turn made it difficult to observe and utilize directly the inverted Lamb-dip resonance in the full-power

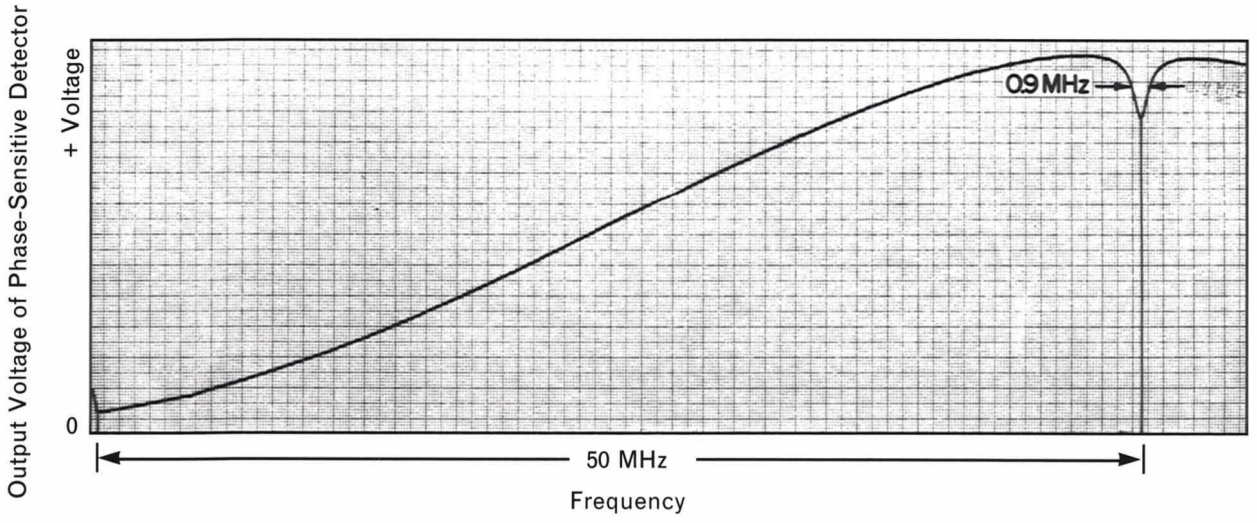

FIGURE 9. Lamb-dip–like appearance of the resonant change in the 4.3-μm fluorescence. The magnitude of the dip is 16.4% of the 4.3-μm fluorescence signal. The pressure in the reference cell was 34 mTorr and the laser power into the cell was 1.75 W in the I-P(20) transition. A frequency dither rate of 260 Hz was applied to the piezoelectric mirror tuner.

output of the CO_2 laser. These difficulties were overcome at Lincoln Laboratory in 1970, when, at the suggestion of A. Javan, we first demonstrated [30, 31] that excellent long-term frequency stability and reproducibility of CO_2 lasers can be readily obtained (and greatly improved upon if necessary) by the frequency stabilization of the lasers to the standing-wave saturation resonance observed in the upper-state-to-ground-state fluorescence of CO_2, as graphically illustrated in Figure 8.

In the experimental procedure, low-pressure room-temperature CO_2 gas that serves as the saturable absorber is subjected to the standing-wave field of the laser cavity, with the laser oscillating in any preselected regular (00^01) or hot-band (01^11) transition. We can detect the saturation effect by observing the change in the intensity of the entire collisionally coupled 4.3-μm spontaneous fluorescence emission band as the laser frequency is tuned across the Doppler profile of the corresponding 10-μm absorption line. In the vicinity of the absorption line center, a resonant change in the 4.3-μm fluorescence signal appears. This standing-wave saturation resonance results from the nonlinearity of the interaction of the standing-wave field in the laser cavity with CO_2 molecules (in the absorption cell) having velocities resonant with the Doppler-shifted frequency of the field as experienced by the molecules. When the laser is tuned to the center frequency of a particular transition ($\omega = \omega_0$), a narrowband ($\Delta f \lesssim 1$ MHz) resonant dip appears in the intensity of the 4.3-μm fluorescence signal. In this case, the traveling-wave components constituting the standing-wave field interact with the same group of CO_2 molecules, namely those molecules which have zero velocity in the direction of the laser's optical axis ($\mathbf{k} \cdot \mathbf{v} = 0$). This resonant change in fluorescence signal is analogous to a Lamb dip.

Figure 9 illustrates the Lamb-dip–like appearance of the resonant change in the 4.3-μm fluorescence signal as the laser is slowly tuned in frequency across the Doppler-broadened gain profile [32]. By applying a small fre-

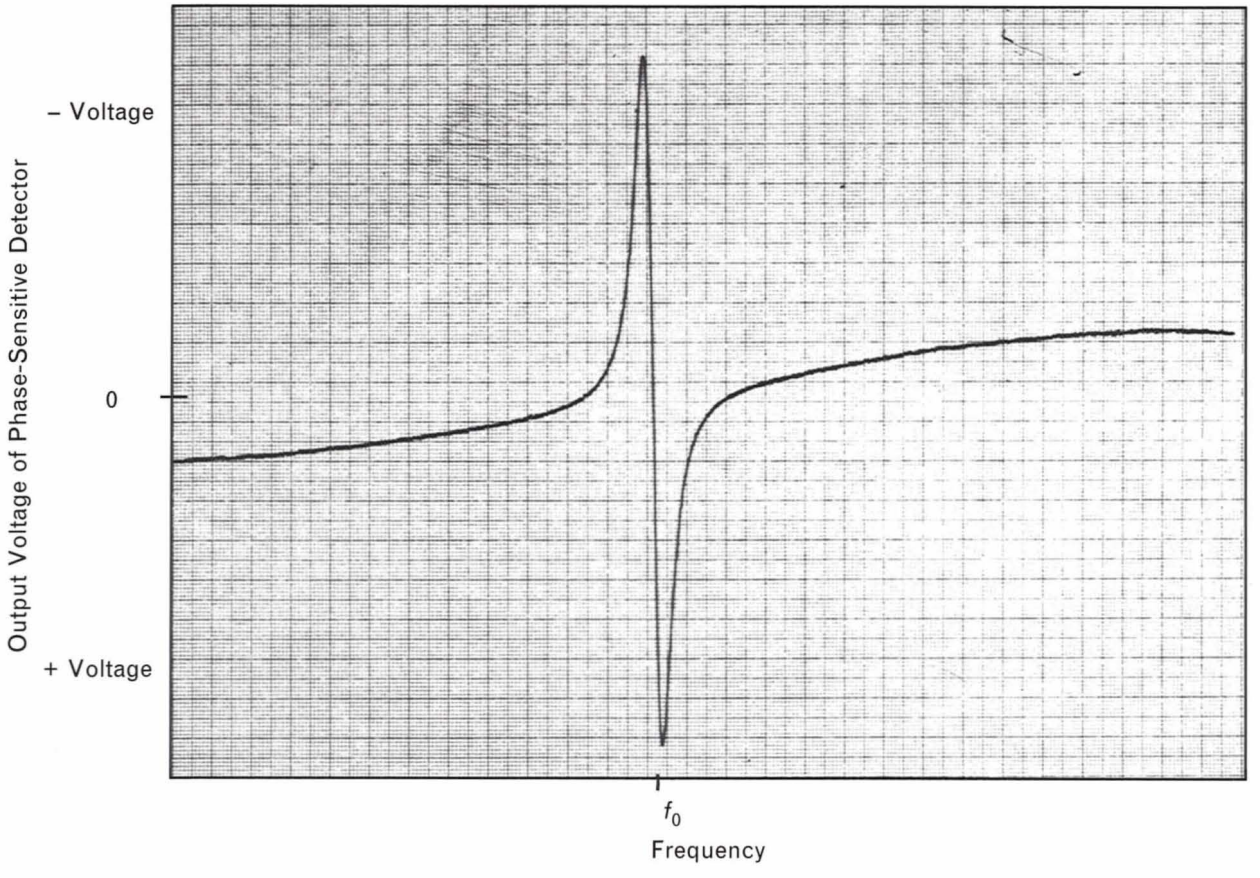

FIGURE 10. Derivative signal at 4.3 μm in the vicinity of the standing-wave saturation resonance shown in Figure 9. SNR ~ 1000, $\Delta f \sim \pm 200$ kHz, and $t = 0.1$ sec (single pole).

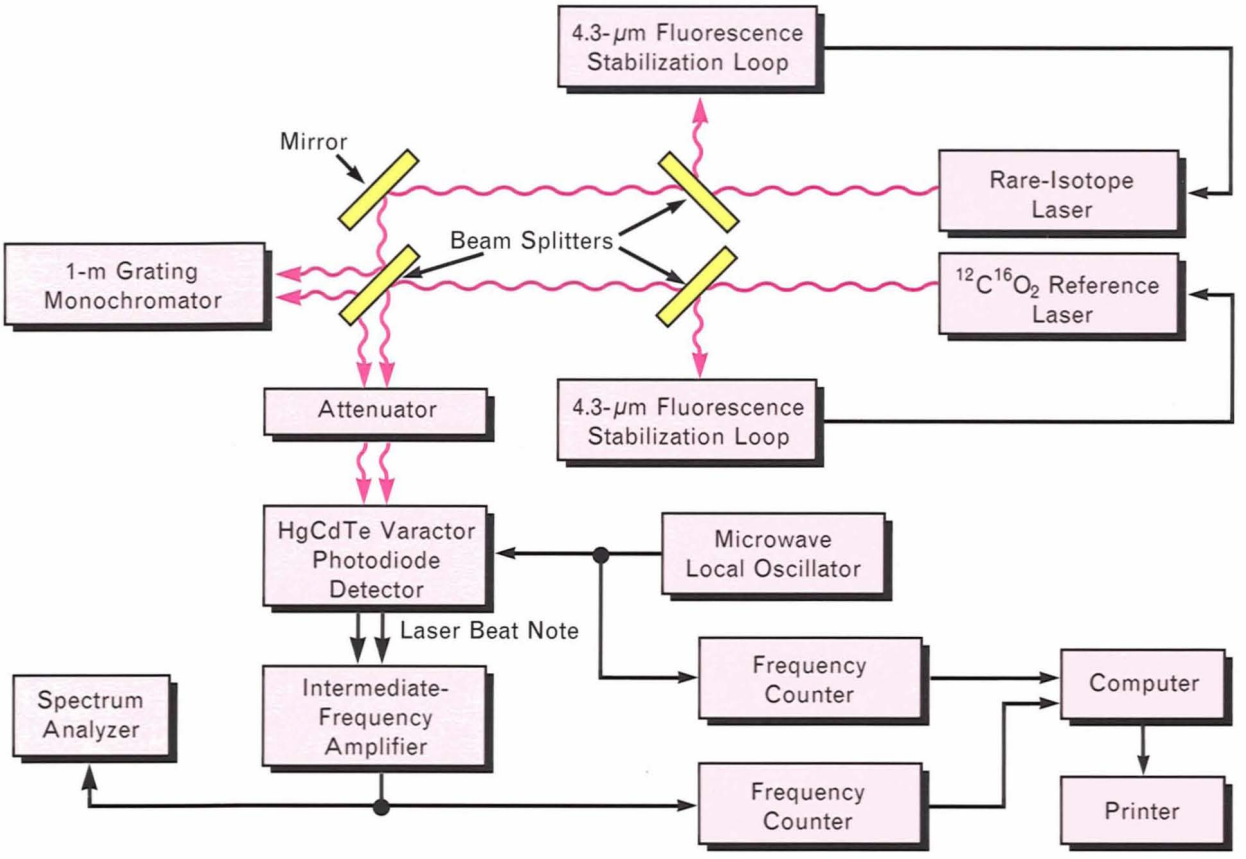

FIGURE 11. Block diagram of the two-channel line-center-stabilized CO_2-isotope calibration system. In the figure, wavy and solid lines denote optical and electrical paths, respectively.

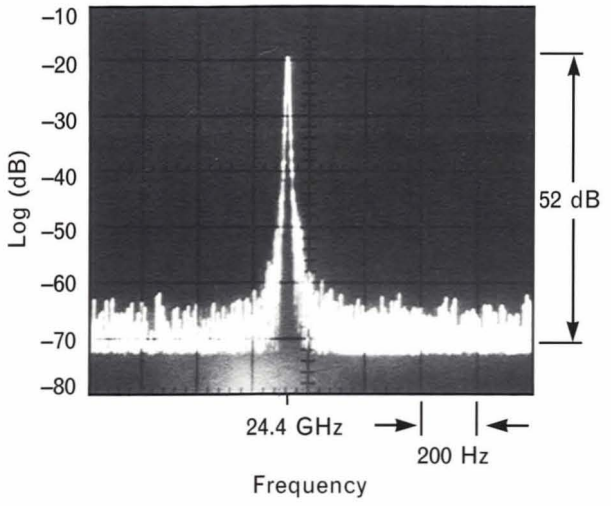

FIGURE 12. The 24.4104191-GHz beat note of a $^{16}O^{12}C^{18}O$ laser I-P(12) transition and a $^{12}C^{16}O_2$ laser I-P(6) transition. The power levels into the photodiode were 0.48 mW for the $^{16}O^{12}C^{18}O$ laser and 0.42 mW for the $^{12}C^{16}O_2$ laser. The second harmonic of the microwave local oscillator was generated in the varactor photodiode. The IF noise bandwidth of the spectrum analyzer was set to 10 kHz.

quency modulation to the laser as it is tuned in the vicinity of the absorption line center, we can obtain the derivative of the 4.3-μm signal [32]. Figure 10, which shows the 4.3-μm derivative signal, was obtained by applying a ±200-kHz frequency modulation to the laser at a 260-Hz rate. A 1.75-W portion of the laser's output was directed into a small external stabilization cell that was filled with pure CO_2 to a pressure of 0.034 Torr at room temperature. It is a straightforward procedure to line-center-stabilize a CO_2 laser through the use of the 4.3-μm derivative signal as a frequency discriminant, in conjunction with a phase-sensitive detector. Any deviation from the center frequency of the lasing transition yields a positive or negative output voltage from the phase-sensitive detector. This voltage is then utilized as a feedback signal in a servoloop to obtain the long-term frequency stabilization of the laser output.

Figure 11 shows a block diagram of a two-channel heterodyne calibration system. In the system, two small, low-pressure, room-temperature CO_2-gas reference cells external to the lasers were used to line-center-stabilize

two grating-controlled stable lasers. The two-channel heterodyne system was used extensively for the measurement and calibration of CO_2-isotope-laser transitions [33, 34].

Figure 12 shows the spectrum-analyzer display of a typical beat note of the system shown in Figure 11. Note that the signal-to-noise ratio (SNR) is greater than 50 dB at the 24.4-GHz beat frequency of the two laser transitions [33].

Figure 13 illustrates the time-domain frequency stability that we have routinely achieved with the two-channel heterodyne calibration system by using the 4.3-μm-fluorescence stabilization technique [34]. The blue solid and hollow circles represent two separate measurement sequences of the Allan variance of the frequency stability

$$\sigma_y(\tau) = \sqrt{\frac{1}{2M}\sum_{j=1}^{M}\left(y_{j+1} - y_j\right)^2}.$$

Each measurement consisted of $M = 50$ consecutive samples for a sample time duration (observation time) of τ seconds. Figure 13 shows that we have achieved $\sigma_y(\tau) < 2 \times 10^{-12}$ for $\tau \sim 10$ sec. Thus a frequency measurement precision of about 50 Hz may be readily achieved within a few minutes.

The triangular symbols in Figure 13 represent the frequency stability of a Hewlett-Packard (HP) model 5061B cesium atomic frequency standard, as specified in the 1990 HP catalog. Clearly, the frequency stabilities of the CO_2- and the cesium-stabilized systems shown in

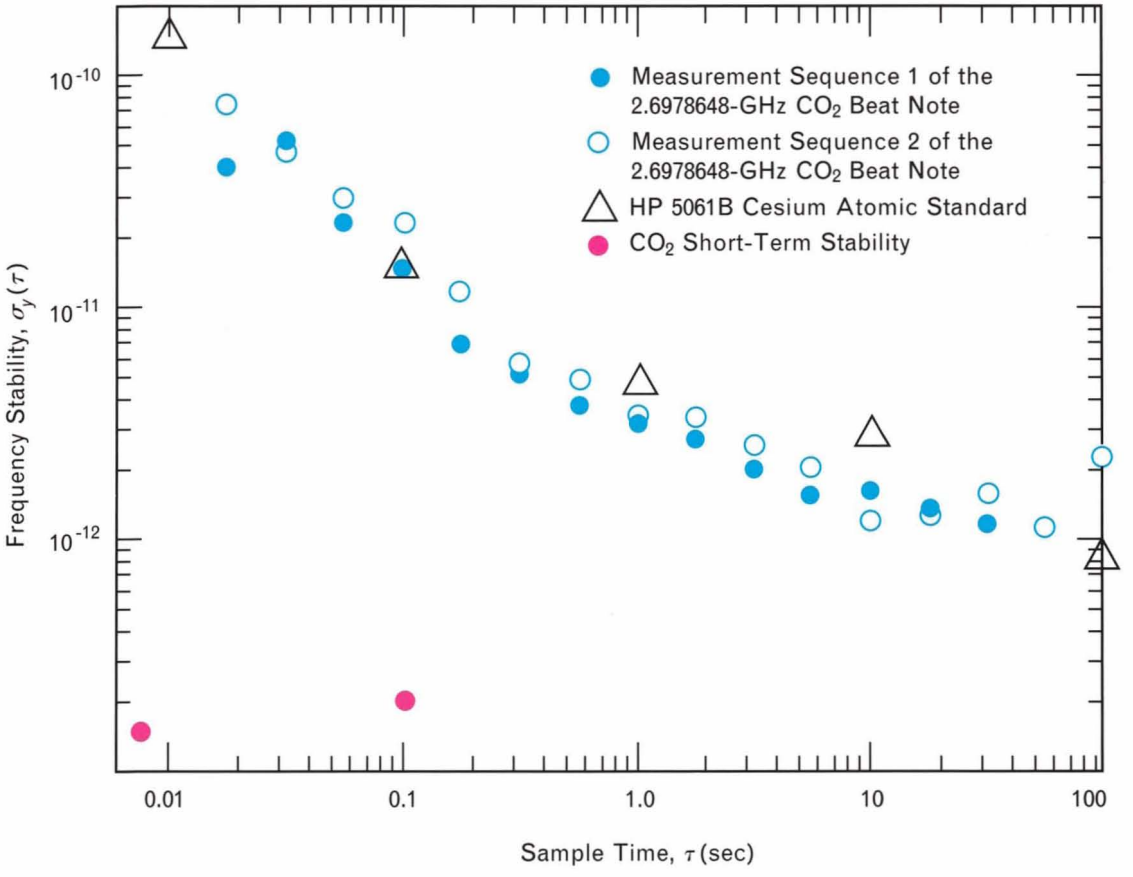

FIGURE 13. Time-domain frequency stability of the 2.6978648-GHz beat note of the $^{13}C^{18}O_2$ laser I-R (24) transition and the $^{12}C^{16}O_2$ reference laser I-P (20) transition in the two-channel heterodyne calibration system (Figure 11) with the 4.3-μm-fluorescence stabilization technique. For the sake of comparison, stabilities of a cesium clock and short-term stabilities of individual CO_2 lasers are also shown. Note that the frequency stabilities of the CO_2- and the cesium-stabilized systems shown are about the same and that the CO_2 radar has achieved short-term stabilities of at least two to three orders of magnitude better than those of microwave systems.

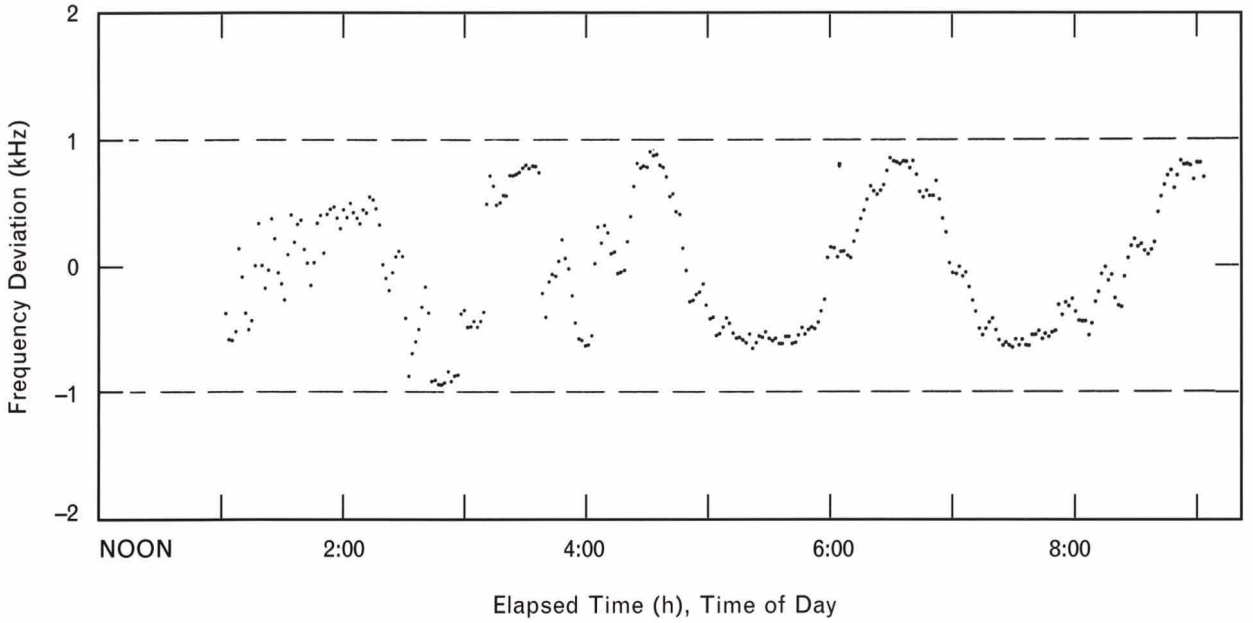

FIGURE 14. Slow drifts in the 2.6978648-GHz beat frequency due to small frequency-offsetting zero-voltage variations of the electronics. The frequency deviations were caused by ambient temperature variations. The beat note was derived from the $^{13}C^{18}O_2$ I-R(24) and the $^{12}C^{16}O_2$ I-P(20) laser transitions. An observation time $\tau = 10$ sec and a sample size of $M = 8$ were used for each data point.

Figure 13 are about the same.

The two magenta circles in the lower left corner of Figure 13 denote the upper bound of the short-term frequency stabilities, as measured in the laboratory (Figure 2) and determined from CO_2 radar returns at the Lincoln Laboratory Firepond Facility (Figure 7). Note that the CO_2 radar has achieved short-term stabilities of at least two to three orders of magnitude better than those of microwave systems.

Figure 14 shows the frequency reproducibility of the two-channel line-center-stabilized CO_2 heterodyne calibration system. The figure contains a so-called drift run that was taken over a period of 8½ hours beginning at 1 PM [34]. The frequency-stability measurement apparatus was fully automatic; it continued to take, compute, and record the beat-frequency data of the two line-center-stabilized CO_2 isotope lasers even at night, when no one was present in the laboratory. Approximately every 100 sec the system printed out a data point that represented the deviation from the 2.6978648-GHz beat frequency, which was averaged over 8½ hours. The system used a measurement time of $\tau = 10$ sec and $M = 8$ samples for each data point, yielding a measurement accuracy much better than the approximately ±1-kHz peak-frequency deviation observable in Figure 14.

The frequency drift was most likely caused by small voltage-offset errors in the phase-sensitive detector-driven servoamplifier outputs that controlled the piezoelectrically tunable laser mirrors. Because 500 V was required to tune the laser one longitudinal mode spacing of 100 MHz, an output voltage error of ±2.5 mV in each channel was sufficient to cause the peak-frequency deviation of ±1 kHz that was observed in Figure 14. By monitoring the piezoelectric drive voltage with the input to the lock-in amplifier terminated with a 50-Ω load (instead of connected to the InSb 4.3-μm fluorescence detector), we determined that slow output-offset voltage drifts of up to ±2.5 mV were indeed present in the electronics. These ±5-ppm zero-voltage drifts were the most probable cause of the ±1-kHz frequency drifts observed in Figure 14. It is important to note that no special precautions were taken to protect either the lasers or the associated electronic circuitry from temperature fluctuations in the laboratory. The fluctuations were substantial—plus or minus several degrees centigrade. Significant improvements are possible with more up-to-date electronics and a temperature-controlled environment; these upgrades will indeed become necessary if the

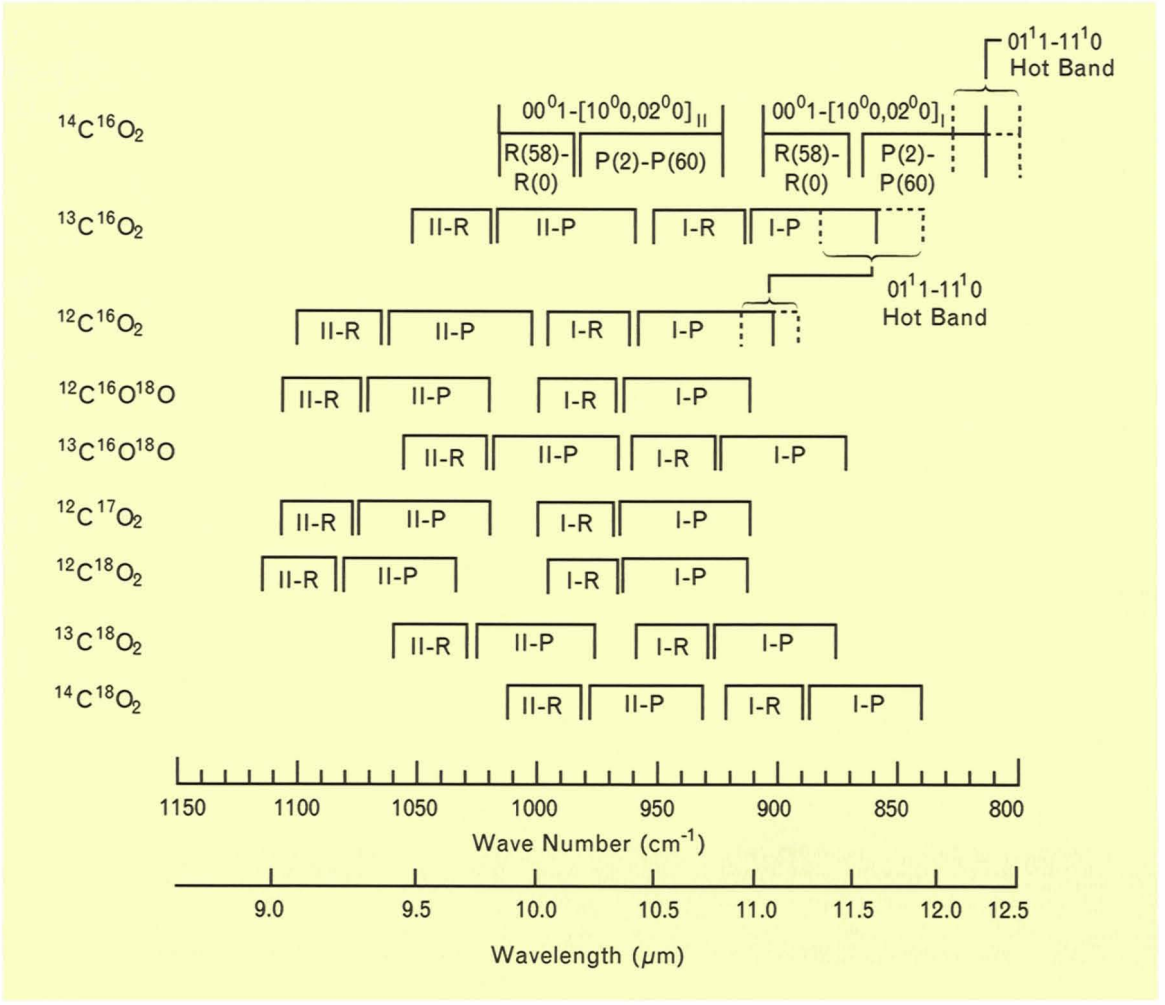

FIGURE 15. Frequency and wavelength domain of lasing transitions in nine CO_2 isotopes.

emphasis changes toward the creation of a primary frequency standard.

Perhaps the greatest advantage of the 4.3-μm fluorescence stabilization method is that it automatically provides a nearly perfect coincidence between the lasing medium's gain profile and the line center of the saturable absorber, because they both utilize the same molecule, CO_2. Thus every P and R transition of the (00^01)-I and -II regular bands and the (01^11) hot band may be line-center-locked with the same stabilization cell and gas fill. Furthermore, as illustrated in Figure 8, the saturation resonance is detected separately at the 4.3-μm fluorescence band and not as a fractional change in the much-higher-power laser radiation at 10 μm. At 4.3 μm, InSb photovoltaic detectors that can provide very high background-limited sensitivity are available.

CO_2-Isotope Lasers as Secondary Frequency Standards

In CO_2 lasers, transitions occur between two vibrational states of the molecule. Because each vibrational state has a whole set of rotational levels, a very large number of laser lines, each with a different frequency (wavelength), can be generated. Moreover, isotopic substitutions of the oxygen and/or carbon atoms make 18 different isotopic combinations possible for the CO_2 molecule. Approximately 80 to 150 regular-band lasing transitions may be generated for each of the CO_2 isotopic species.

Through the use of optical heterodyne techniques, beat frequencies between laser transitions of individually line-center-stabilized CO_2-isotope lasers in pairs were accurately measured. As a result, the absolute frequen-

cies, vacuum wave numbers, band centers, and rotational-vibrational molecular constants for $^{12}C^{16}O_2$, $^{13}C^{16}O_2$, $^{13}C^{18}O_2$, $^{12}C^{18}O_2$, $^{12}C^{17}O_2$, $^{16}O^{12}C^{18}O$, $^{16}O^{13}C^{18}O$, $^{14}C^{16}O_2$, and $^{14}C^{18}O_2$ were simultaneously calculated from well over 900 beat-frequency measurements [35, 36]. The accuracies of these frequency determinations were, for the majority of the transitions, within about 5 kHz relative to the primary Cs frequency standard [36]. Consequently, in the wavelength region of 8.9 to 12.3 μm, line-center-stabilized CO_2-isotope lasers can be conveniently used as secondary frequency standards.

Figure 15 graphically illustrates the frequency and wavelength domain of the nine CO_2 isotopic species that have been measured to date. $^{14}C^{16}O_2$ extends the wavelength range to well beyond 12 μm; $^{12}C^{18}O_2$ transitions can reach below 9 μm. It should be noted that the frequency tables generated and published by Lincoln Laboratory have been extensively employed and reprinted in several publications and books in the United States and other countries.

We can also utilize harmonics and the difference frequencies of CO_2 lasing transitions to synthesize precisely known reference frequencies well beyond the 8.9-to-12.3-μm range of the CO_2-isotope-laser transition frequencies illustrated in Figure 15. For instance, heterodyne comparisons with the second harmonics of appropriately selected CO_2 laser transitions have achieved the first accurate determination of several CO-isotope laser lines in the 5-to-6-μm range [37]. Table 1, which demonstrates infrared (IR) synthesis at 16 μm (625 cm^{-1}) [38, 39], is another example. To generate Table 1, we gave a computer the task of finding the CO_2-isotope-laser transitions for which the difference frequencies between a frequency-doubled $^{14}C^{16}O_2$-laser transition and any other CO_2-isotope-laser transition fell within the 625.0 ±0.1 cm^{-1} frequency range. Synthesized frequency tables very similar to Table 1 have been used for the accurate determination of absorption lines in isotopes of uranium hexafluoride (UF_6) near 16 μm.

Figure 16 illustrates a calibration method for locating and precisely calibrating reference lines that can be easily

Table 1. An Example of IR Synthesis at 16 μm with Regular-Band CO_2 Transitions

Wave Number = (2 × Transition 1) – (Transition 2)		
Wave Number (cm^{-1})	Transition 1	Transition 2
624.906042	$^{14}C^{16}O_2$ I-P (40)	$^{13}C^{16}O_2$ II-R (30)
624.915792	$^{14}C^{16}O_2$ I-P (28)	$^{12}C^{16}O^{18}O$ II-P (16)
624.917820	$^{14}C^{16}O_2$ I-P (48)	$^{12}C^{16}O^{18}O$ II-P (56)
624.937049	$^{14}C^{16}O_2$ I-P (56)	$^{13}C^{18}O_2$ II-P (26)
624.945145	$^{14}C^{16}O_2$ I-P (14)	$^{12}C^{16}O^{18}O$ II-R (16)
624.954490	$^{14}C^{16}O_2$ I-P (4)	$^{12}C^{18}O_2$ II-R (26)
624.978786	$^{14}C^{16}O_2$ I-P (48)	$^{13}C^{16}O_2$ II-R (6)
624.988389	$^{14}C^{16}O_2$ I-P (20)	$^{12}C^{16}O^{18}O$ II-R (1)
625.007851	$^{14}C^{16}O_2$ I-P (16)	$^{12}C^{18}O_2$ II-P (4)
625.013741	$^{14}C^{16}O_2$ I-P (6)	$^{12}C^{16}O_2$ II-R (56)
625.044477	$^{14}C^{16}O_2$ I-P (2)	$^{12}C^{16}O^{18}$II-R (52)
625.046863	$^{14}C^{16}O_2$ I-P (54)	$^{14}C^{18}O_2$ II-R (52)
625.091263	$^{14}C^{16}O_2$ I-P (4)	$^{12}C^{16}O^{18}O$ II-R (45)

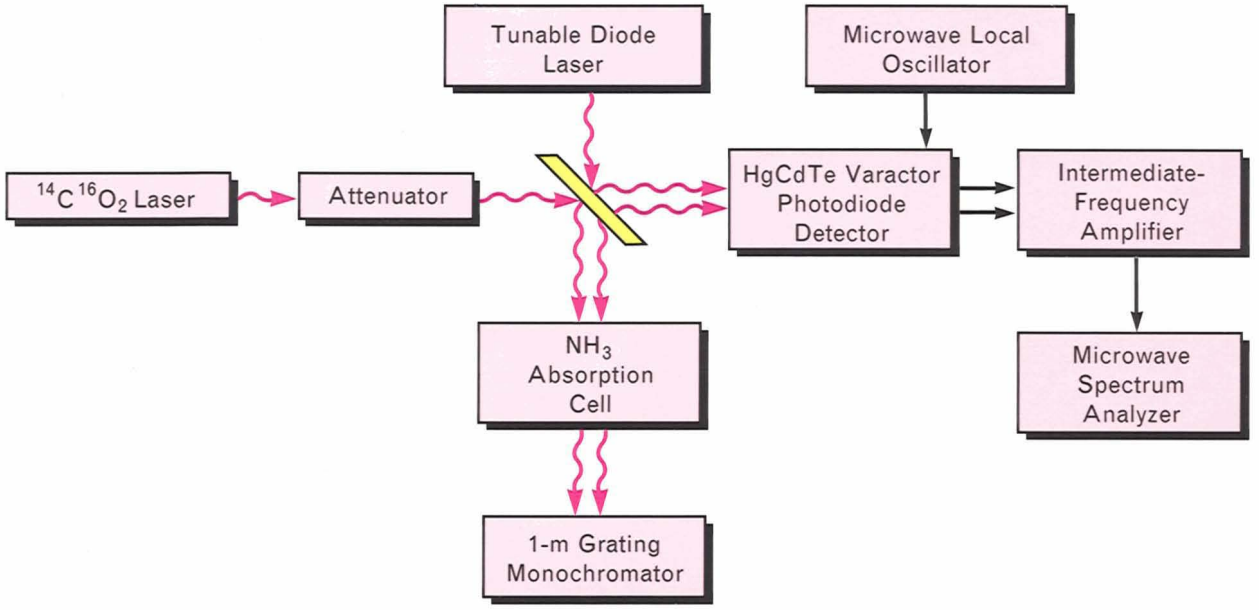

FIGURE 16. High-accuracy calibration method for heterodyne spectroscopy with tunable lasers. In the figure, wavy and solid lines denote optical and electrical paths, respectively.

used to determine the absorption spectra of UF_6 isotopes in the vicinity of 12 μm [38, 39]. In the experimental arrangement, a beam splitter combines the output of a tunable lead-salt diode laser and that of a $^{14}C^{16}O_2$ laser. A fast HgCdTe varactor photodiode [40] heterodynes one part of the combined radiation, the beat note of which is displayed and measured by a microwave spectrum analyzer (or frequency counter). The other part of the combined laser radiation is used to probe an absorption cell that, in this particular experiment, is filled with NH_3 gas at a pressure of 5 Torr. With the CO_2 laser stabilized to its line center and the diode laser locked to the absorption line to be measured, heterodyne calibration provides an accuracy not currently available by any other method. As an example, Figure 17 shows a heterodyne beat frequency of 6775 MHz between a $^{14}C^{16}O_2$ laser and a diode laser tuned to one of the NH_3 absorption lines near 12.1 μm.

In another project at Lincoln Laboratory, we demonstrated the equivalent of a programmable and highly accurate tunable IR synthesizer, as shown in Figure 18 [41, 42]. In the figure, the IR synthesizer output is derived from a lead-salt tunable diode laser (TDL); a small portion of the TDL output is heterodyned against a line-center-stabilized grating-controlled CO_2 or CO molecular laser. A high-speed HgCdTe varactor photodiode detects the beat note of the two lasers. The detected beat frequency, which is generally in the 0-to-18-GHz range, is further heterodyned to some convenient intermediate frequency (IF) through the use of readily available commercial RF/microwave-frequency synthesizers and wideband double-balanced mixers. The IF output is amplified and amplitude limited by means of low-noise wideband amplifiers and limiters. The limiter output is, in turn, used as input to a wideband delay-line type of frequency discrimi-

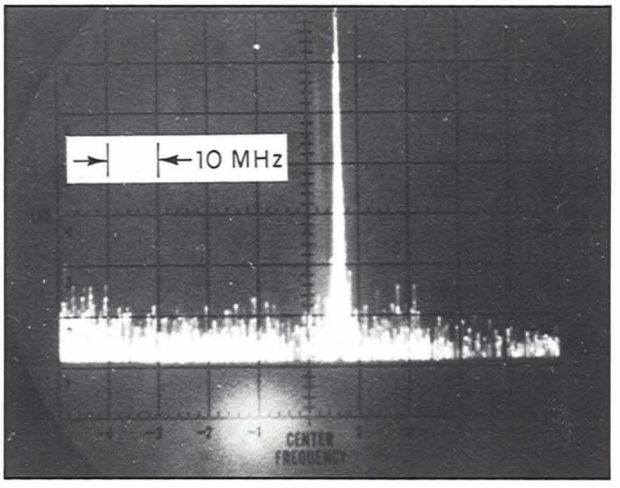

FIGURE 17. The 6775-MHz beat note of a $^{14}C^{16}O_2$-laser 00^01-[10^00, 02^00] I-band P-transition and a diode laser tuned to an ammonia absorption line at 12.1 μm.

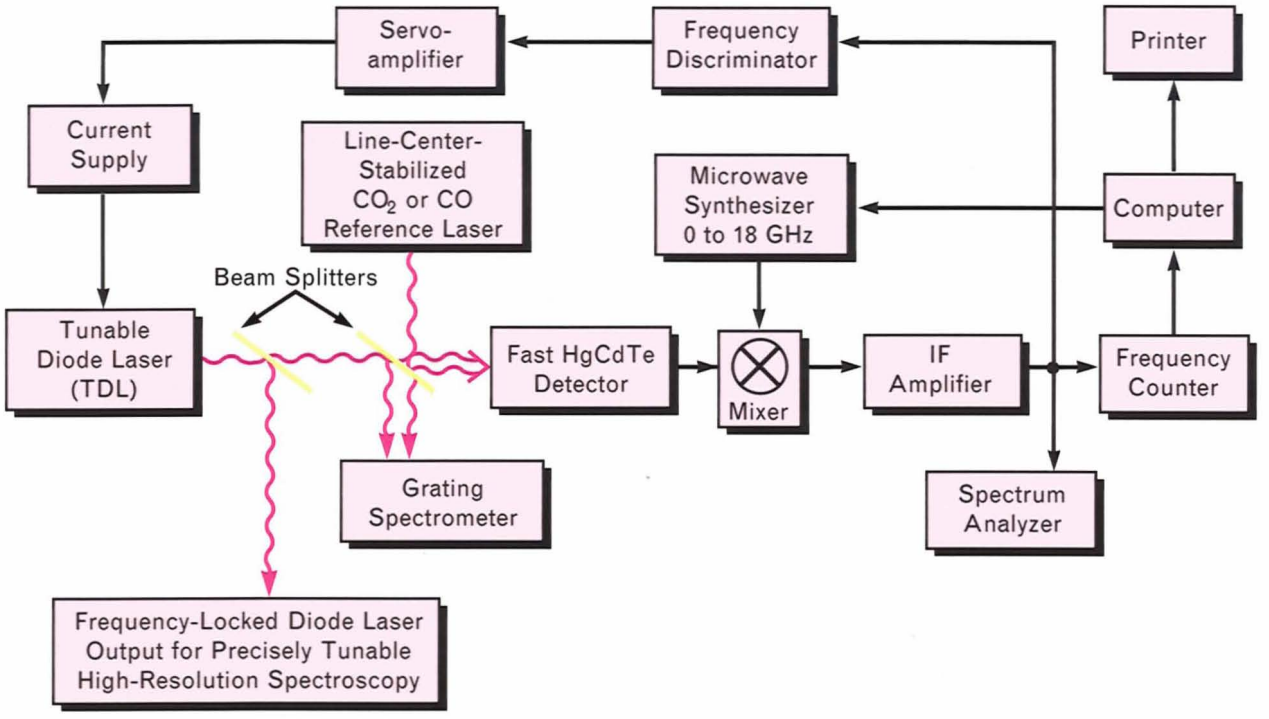

FIGURE 18. Block diagram of an accurate, continuously tunable, computer-controlled, kilohertz-resolution infrared-frequency synthesizer.

nator (200-to-600-MHz typical bandwidth).

A servoamplifier/integrator further amplifies the output of the frequency discriminator, and the amplified output is then used to control the TDL current, which determines the TDL output frequency. Closing the servoloop in this fashion frequency-offset-locks the TDL output to the combination of CO_2 (or CO) laser, RF/microwave synthesizer, and the center frequency of the wideband IF discriminator, which a frequency counter accurately monitors.

A computer controls the entire infrared synthesizer system shown in Figure 18. If, for instance, the microwave synthesizer is frequency swept under computer control, the IR output frequency of the TDL would also be swept in synchronism with the microwave synthesizer because the frequency-offset-locking servoloop forces the TDL output to maintain the following frequency relationship:

$$f_{\mathrm{TDL}} = f_{\mathrm{CO_2/CO}} \pm f_{\mathrm{synthesizer}} \pm f_{\mathrm{IF\ counter}} . \quad (2)$$

Either the operator or the computer program predetermines the frequency of the RF/microwave synthesizer in Equation 2. The IF is very accurately measured, and averaged if so desired, even in the presence of appreciable frequency modulation, which may be necessary to line-center-lock either one or both lasers. Thus to a great extent the absolute accuracy of the TDL output frequency f_{TDL} will depend only on the absolute accuracy, resettability, and long-term stability of the reference molecular gas laser(s). To date, the most accurate results have been achieved with the use of CO_2 reference lasers.

Laser Design

Most of the stable gas-laser oscillators we designed and constructed at Lincoln Laboratory have several common features, described as follows.

A nearly semi-confocal optical-cavity configuration is used, which yields a ratio of relative diffraction loss of about 10 to 1 between the low-loss off-axis TEM_{10q} mode and the desired fundamental TEM_{00q} mode. In general, only fundamental TEM_{00q}-mode operation can overcome the combined losses, which are due to output coupling and diffraction. The lasers are dc-excited internal-mirror tubes in which four invar alloy rods rigidly space the mirror holders to achieve maximum open-loop stability.

Figure 19 is a photograph of the first stable CO_2 laser built at Lincoln Laboratory. This laser also bears the closest resemblance to the Javan design. As mentioned

in the introduction, this particular laser is a modified version of the He-Ne lasers used in previous experiments. The modifications involved changing two mirrors and the output window, and substituting a water-cooled discharge tube with a cold (not thermionic) cathode. In addition, a differential-screw tuning mechanism was affixed to one of the mirror holders to permit a 3.5-μm-per-turn axial motion of one of the laser mirrors [26].

The next set of lasers, built for the CO_2 radar at Firepond, were in most respects similar to the one shown in Figure 19, except that superinvar rods with very low coefficients of expansion were used for the optical-cavity spacers [26]. To the best of the author's knowledge, this was the first use of superinvar for the optical resonator of a laser. Furthermore, acoustic damping, magnetic shielding, and thermal insulation of the optical cavity was achieved by a variety of materials surrounding each superinvar rod in a concentrically layered arrangement. Viscous damping compounds, insulating foam, lead, Mu metal and Co-netic shields, and aluminum foil provided this isolation of the rods. The shielded superinvar cavity lasers yielded an additional factor-of-100 improvement in short-term stability [26] compared to the first two CO_2 lasers shown in Figure 19.

The above lasers were soon replaced by a family of completely redesigned third-generation CO_2 lasers, which have been in use at Lincoln Laboratory since the beginning of 1968 [18]. In the new design, careful choice of materials and techniques are employed for further enhancing the open-loop stability of the optical cavity. However, in spite of the rigid structure, the laser design is entirely modular and can be rapidly disassembled and reassembled; mirrors can be interchanged, and mirror holders can be replaced by piezoelectric and grating-controlled tuners. The stainless steel endplates and the eight differential-alignment screws (Figure 19) have been replaced by much more stable black diabase endplates and a novel internal mirror-alignment mechanism that is not accessible from the outside. The new lasers are not only more stable, but also much easier to align and less costly to manufacture.

All the results described in the previous three sections of this article were obtained with the third-generation CO_2 lasers described above. The remainder of this section will show photographs of several variants of these lasers and some of the experimental setups previously given in block-diagram forms.

Figure 20 illustrates the simplest configuration: the laser has two mirrors, one of which is piezoelectrically tunable. Two-mirror lasers come in various lengths, depending on the output-power requirement.

Four two-mirror lasers (lengths of 50, 50, 150, and 236 cm) are contained in Figure 21. The figure shows the vault that contains the various isotopic CO_2 local and power oscillators for the optical radar at the Lincoln

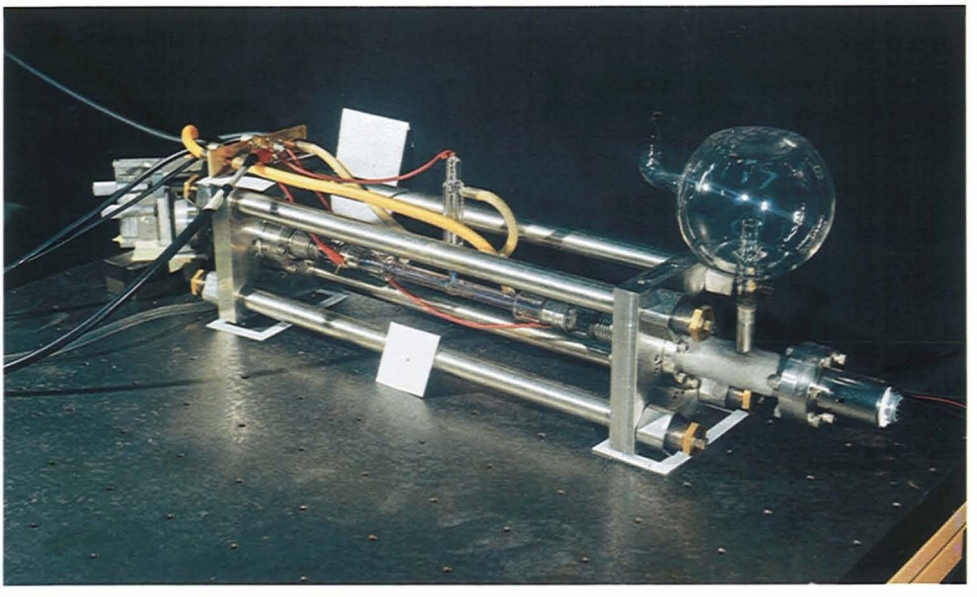

FIGURE 19. The first stable CO_2 laser built at Lincoln Laboratory.

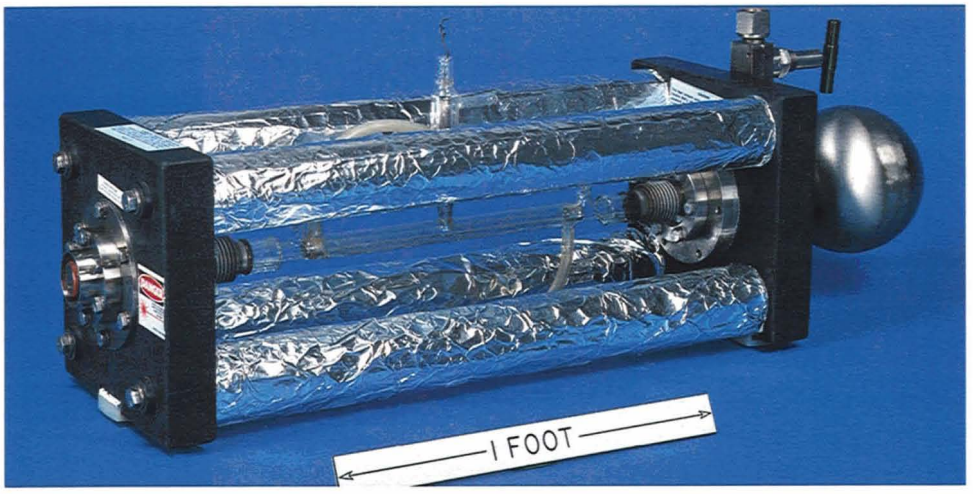

FIGURE 20. Basic two-mirror ultrastable laser.

Laboratory Firepond Facility. A fifth, grating-controlled laser can also be seen in the figure.

Figure 22 is a close-up photograph of a grating-controlled stable TEM_{00q}-mode laser. Many variants of this basic design exist both at Lincoln Laboratory and elsewhere. This particular unit was built for a relatively high-power application such as optical pumping and frequency shifting. In the laser shown in Figure 22 the first-order reflection of the grating was coupled through a partially reflecting output mirror. For heterodyne spectroscopy, zero-order output coupling from the grating is preferable because many more laser transitions can be obtained with such lasers.

Three grating-controlled lasers with zero-order output coupling are contained in Figure 23, a photograph of the two-channel heterodyne measurement system of

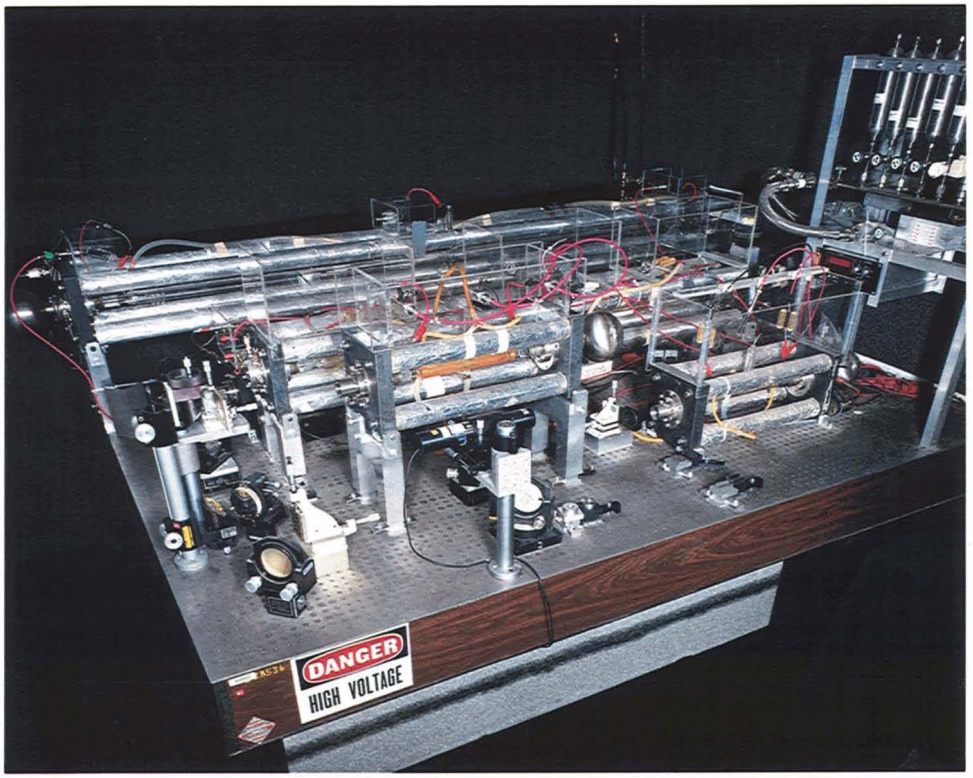

FIGURE 21. CO_2-isotope lasers in the oscillator vault of the Firepond radar.

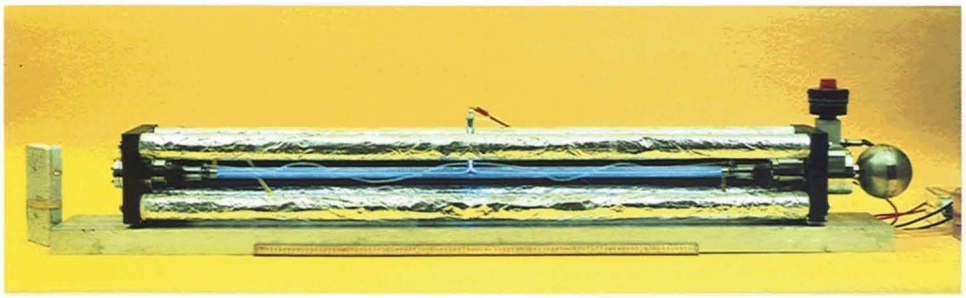

FIGURE 22. Basic grating-controlled stable TEM_{00q}-mode CO_2 laser.

Figure 11. The two external frequency-stabilization cells, used for the individual line-center locking of lasers in pairs, are also clearly visible in Figure 23.

Some of the lasers have short intracavity absorption cells that can be used either for frequency stabilization or for very stable high-repetition-rate passive Q-switching. Figure 24 shows a 50-cm two-mirror laser with a short (3 cm) internal absorption cell. This laser was the one with which the 4.3-μm standing-wave saturation resonance and the subsequent line-center stabilization of a CO_2 laser were first demonstrated through the use of the 4.3-μm fluorescence signal at Lincoln Laboratory in 1970 [30, 31]. The line-center locking of CO_2-isotope lasers with the 4.3-μm fluorescence technique has been used in all countries (including the United States) that have set up laser chains to tie the frequency of visible lasers to the microwave cesium frequency standard.

The third-generation CO_2/CO lasers described above and shown in the last five figures are members of the same family because most of the parts used in them are completely interchangeable. Thus a new laser can be built or completely reconfigured with spare parts in a very short period of time, usually within a few hours.

For more than two decades the dual requirements of modularity of laser design and interchangeability of parts have provided a vast amount of convenience and

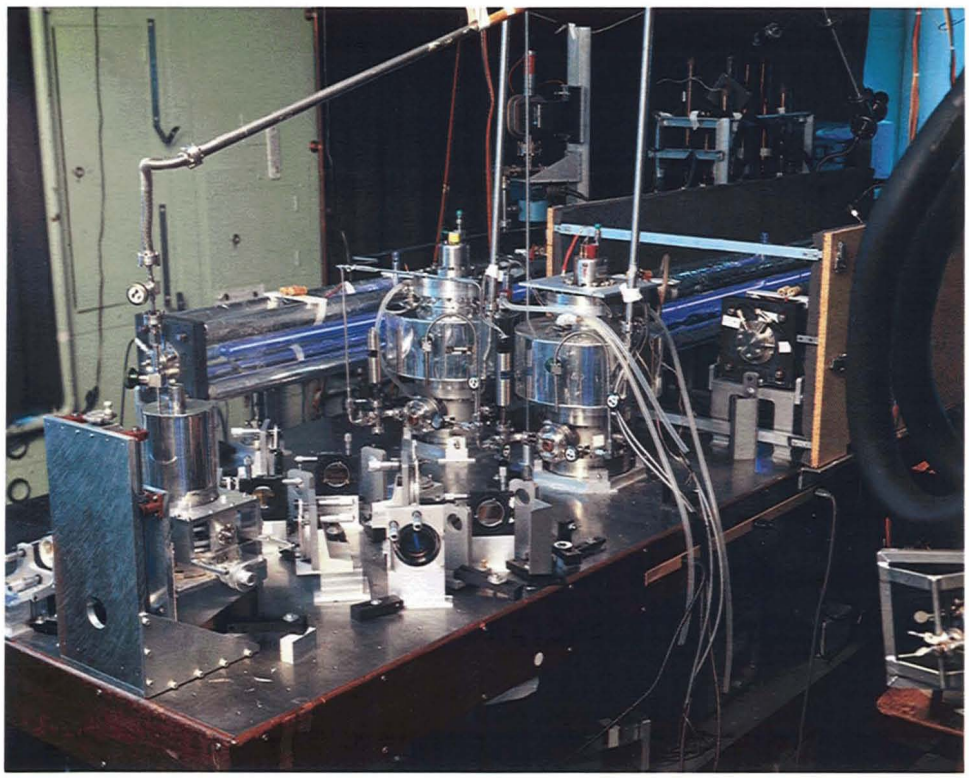

FIGURE 23. The optical portion of the two-channel CO_2 calibration system.

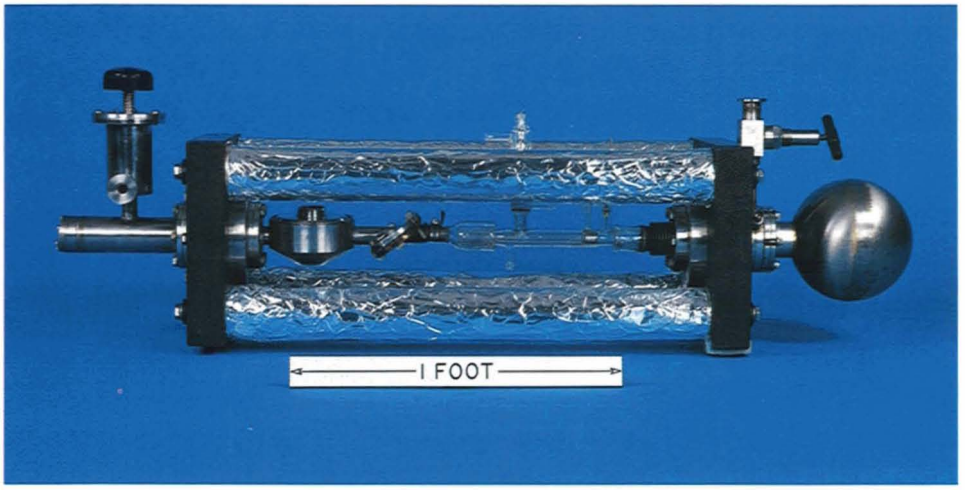

FIGURE 24. Two-mirror stable laser with short intracavity cell. This laser was used for the first demonstration of the standing-wave saturation resonance observed via the 4.3-μm fluorescence signal.

savings both in time and cost. But such requirements have perforce introduced certain limitations in design and performance. Thus, if the need to do so arises, we could improve both short-term stability and long-term stabilization of the lasers with relative ease by putting less emphasis on modularity and interchangeability. Indeed, several years ago we prepared certain changes in design and even procured some of the components for this purpose. However, the instrumentation currently available is not sufficient to measure definitively even the stabilities of our present lasers.

Conclusions

CO_2 lasers have demonstrated greater spectral purity and better short-term stability than any other currently available oscillator at any frequency. This statement has been confirmed by laboratory measurements and by the analysis of CO_2-laser radar returns from orbiting satellites. Furthermore, we also invented and developed at MIT/Lincoln Laboratory a highly effective long-term stabilization technique that can use low-pressure room-temperature CO_2 gas as a reference; the technique has achieved long-term CO_2-laser stabilities at least comparable to commercial-grade atomic clocks. A line-center-stabilized two-channel CO_2-laser heterodyne calibration system was used to determine the absolute frequencies of lasing transitions and the rotational-vibrational molecular constants of nine CO_2 isotopic species to within about 5 kHz relative to the primary cesium frequency standard. These results have enabled usage of the CO_2 system as the most precise secondary frequency standard currently available in the infrared spectral region.

It should be noted that the results described in this article were achieved with laser designs and components that were developed more than 20 years ago. Extensive experience gained by working with these lasers clearly indicates that updated designs could easily improve the short-term and long-term stabilities by at least one to two orders of magnitude.

Acknowledgments

The work reported in this article is the result of the active encouragement and cumulative efforts of many individuals in the MIT/Lincoln Laboratory community. In particular, the author thanks the contributions of the following individuals (listed in alphabetical order): J.W. Bielinski, L.C. Bradley, J.A. Daley, T.R. Gurski, H.A. Haus, A. Javan, R.H. Kingston, D.G. Kocher, R.G. O'Donnell, K.L. SooHoo, D.L. Spears, L.J. Sullivan, J.E. Thomas, and C.H. Townes.

REFERENCES

1. C.K.N. Patel, "Continuous-Wave Laser Action on Vibrational-Rotational Transitions of CO_2," *Phys. Rev.* **136**, A1187 (1964).
2. C.K.N. Patel, "Vibration Energy Transfer—An Efficient Means of Selective Excitation in Molecules," in *Physics of Quantum Electronics Conference Proceedings*, eds. P.L. Kelley,

B. Lax, and P.E. Tannenwald (McGraw-Hill, 1966), pp. 643–654.
3. R.H. Kingston and L.J. Sullivan, "Coherent Laser Radar," in *Proc. SPIE: 19th Annual Intl. Tech. Symp. on Optical Design Problems in Laser Systems* **69,** 10 (1975).
4. L.J. Sullivan, "Infrared Coherent Radar," *Proc. SPIE: CO_2 Laser Devices and Applications* **227,** 148 (1980).
5. L.J. Sullivan, B.E. Edwards, and W.E. Keicher, "The Firepond High Power Carbon Dioxide Laser Radar System," *Proc. Intl. Conf. on Radar, Paris, 24–28 Apr. 1989,* p. 353.
6. " 'Firefly' Laser Experiment Successful in Measuring Inflatable Decoy Motion," *Aviat. Week Space Technol.,* p. 75 (23 Apr. 1990).
7. A. Javan, W.B. Bennett, Jr., and D.R. Herriott, "Population Inversion and Continuous Optical Maser Oscillation in a Gas Discharge Containing a He-Ne Mixture," *Phys. Rev. Lett.* **6,** 106 (1961).
8. T.S. Jaseja, A. Javan, and C.H. Townes, "Frequency Stability of He-Ne Masers and Measurements of Length," *Phys. Rev. Lett.* **10,** 165 (1963).
9. C.H. Townes, "Some Applications of Optical and Infrared Masers" in *Advances in Quantum Electronics,* ed. J.R. Singer (Columbia University Press, New York, 1961), p. 11.
10. L. Mandel and E. Wolf, eds., *Selected Papers on Coherence and Fluctuations of Light* (Dover Publications, New York, 1970).
11. J.A. Bellisio, C. Freed, and H.A. Haus, "Noise Measurements on He-Ne Laser Oscillators," *Appl. Phys. Lett.* **4,** 5 (1964).
12. C. Freed and H.A. Haus, "Measurement of Amplitude Noise in Optical Cavity Masers," *Appl. Phys. Lett.* **6,** 85 (1965).
13. C. Freed and H.A. Haus, "Photocurrent Spectrum and Photoelectron Counts Produced by a Gaseous Laser," *Phys. Rev.* **141,** 287 (1966).
14. C. Freed and H.A. Haus, "Photoelectron Statistics Produced by a Laser Operating below the Threshold of Oscillation," *Phys. Rev. Lett.* **15,** 943 (1965).
15. C. Freed and H.A. Haus, "Amplitude Noise in Gas Lasers below and above the Threshold of Oscillation," in *Physics of Quantum Electronics Conference Proceedings,* eds. P.L. Kelley, B. Lax, and P.E. Tannenwald (McGraw-Hill, 1966), pp. 715–724.
16. C. Freed and H.A. Haus, "Photoelectron Statistics Produced by a Laser Operating below and above the Threshold of Oscillation," *IEEE J. Quant. Electron.* **QE-2,** 190 (1966).
17. C. Freed, "Stability Measurements of CO_2-N_2-He Lasers at 10.6 μm Wavelength," *IEEE J. Quant. Electron.* **QE-3,** 203 (1967).
18. C. Freed, "Designs and Experiments Relating to Stable Gas Lasers," in *Proc. Frequency Standards and Metrology Seminar, National Research Council of Canada and Université Laval, Quebec, Canada, 30 Aug.–1 Sept. 1971,* p. 226.
19. C. Freed, "Sealed-Off Operation of Stable CO Lasers," *Appl. Phys. Lett.* **18,** 458 (1971).
20. C. Freed and H.A. Haus, "Lamb Dip in CO Lasers," *IEEE J. Quantum Electron.* **QE-9,** 219 (1973).
21. A.L. Betz, M.A. Johnson, R.A. McLaren, and E.C. Sutton, "Heterodyne Detection of CO_2 Emission Lines and Wind Velocities in the Atmosphere of Venus," *Astrophys. J.* **208,** pt. 2, L141 (15 Sept. 1976).
22. M.A. Johnson, A.L. Betz, R.A. McLaren, and C.H. Townes, "Nonthermal 10 Micron CO_2 Emission Lines in the Atmospheres of Mars and Venus," *Astrophys. J.* **208,** pt. 2, L145 (15 Sept. 1976).
23. A.L. Schawlow and C.H. Townes, "Infrared and Optical Masers," *Phys. Rev.* **112,** 1940 (1958).
24. T.H. Maiman, "Stimulated Optical Radiation in Ruby," *Nature* **187,** 493 (Aug. 1960).
25. E.D. Hinkley and C. Freed, "Direct Observation of the Lorentzian Line Shape as Limited by Quantum Phase Noise in a Laser above Threshold," *Phys. Rev. Lett.* **23,** 277 (1969).
26. C. Freed, "Design and Short-Term Stability of Single-Frequency CO_2 Lasers," *IEEE J. Quant Electron.* **QE-4,** 404 (1968).
27. C. Freed, "Progress in CO_2 Laser Stabilization," in *Proc. 31st Annual Symp. on Frequency Control, Atlantic City, NJ, 1–3 June 1977.*
28. C. Freed, "Ultrastable Carbon Dioxide (CO_2) Lasers," in *Proc. SPIE: Laser Research and Development in the Northeast* **709,** 36 (1986).
29. T.R. Gurski, "Laser Frequency Stability Limitations on a 10.6 μm Laser Radar," *J. Opt. Soc. Am.* **66,** 1133A (1976).
30. C. Freed and A. Javan, "Standing-Wave Saturation Resonances in the CO_2 10.6-μ Transitions Observed in a Low-Pressure Room-Temperature Absorber Gas," *Appl. Phys. Lett.* **17,** 53 (1970).
31. A. Javan and C. Freed, "Method of Stabilizing a Gas Laser," U.S. Patent No. 3686585, issued 22 Aug. 1972.
32. C. Freed and R.G. O'Donnell, "Advances in CO_2 Laser Stabilization Using the 4.3 μm Fluorescence Technique," *Metrologia* **13,** 151 (1977).
33. C. Freed, "Frequency Stabilization of CO_2 Lasers," in *Proc. 29th Annual Symp. on Frequency Control, Atlantic City, NJ, 28–30 May 1975.*
34. K.L. SooHoo, C. Freed, J.E. Thomas, and H.A. Haus, "Line-Center Stabilized CO_2 Lasers as Secondary Frequency Standards: Determination of Pressure Shifts and Other Errors," *IEEE J. Quant. Electron.* **QE-21,** 1159 (1985).
35. C. Freed, L.C. Bradley and R.G. O'Donnell, "Absolute Frequencies of Lasing Transitions in Seven CO_2 Isotopic Species," *IEEE J. Quant. Electron.* **QE-16,** 1195 (1980).
36. L.C. Bradley, K.L. SooHoo, and C. Freed, "Absolute Frequencies of Lasing Transitions in Nine CO_2 Isotopic Species," *IEEE J. Quant. Electron.* **QE-22,** 234 (1986).
37. R.S. Eng. H. Kildal, J.C. Mikkelsen, and D.L. Spears, "Determination of Absolute Frequencies of $^{12}C^{16}O$ and $^{13}C^{16}O$ Laser Lines," *Appl. Phys. Lett.* **24,** 231 (1974).
38. C. Freed, "Status of CO_2 Isotopic Laser Technology," *Proc. Intl. Conf. on Lasers, New Orleans, 15–19 Dec. 1980.*
39. C. Freed, "Status of CO_2 Isotope Lasers and Their Applications in Tunable Laser Spectroscopy," *IEEE J. Quant. Electron.* **QE-18,** 1220 (1982).
40. D.L. Spears and C. Freed, "HgCdTe Varactor Photodiode Detection of CW CO_2 Laser Beats beyond 60 GHz," *Appl. Phys. Lett.* **23,** 445 (1973).
41. C. Freed, J.W. Bielinski, and W. Lo, "Programmable, Secondary Frequency Standard Based Infrared Synthesizer Using Tunable Lead-Salt Diode Lasers," in *Proc. SPIE: Tunable Diode Laser Development and Spectroscopy Applications* **438,** 119 (1983).
42. C. Freed, "Programmable, Secondary Frequency Standards Based Infrared Synthesizers for High Resolution Spectroscopy," in *Methods of Laser Spectroscopy,* eds. Y. Prior, A. Ben-Reuven, and M. Rosenbluh (Plenum Press, New York, 1986), pp. 151–161.

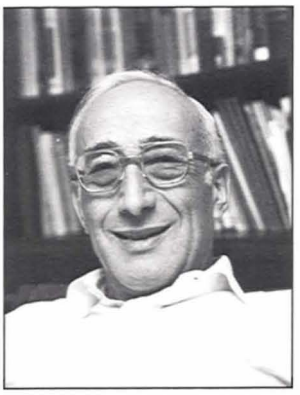

CHARLES FREED
was born in Budapest, Hungary, in 1926. He received a B.E.E. degree from New York University in 1952, and S.M. and E.E. degrees in electrical engineering from MIT in 1954 and 1958, respectively.

From 1952 to 1958 Charles was employed by the Research Laboratory of Electronics at MIT as a research assistant and staff member. He later worked at Raytheon Company's Spencer Laboratory, Special Microwave Devices Operation, and Research Division. He joined Lincoln Laboratory as a staff member in February 1962, and became a member of the senior staff in 1978. Since 1969 he has also been a lecturer in the Department of Electrical Engineering and Computer Science at MIT.

He has written numerous technical papers on a variety of topics, including microwave noise on electron beams; varactor diode parametric amplifiers; amplitude noise and photoelectron statistics of He-Ne lasers; the frequency stability, design, and output characteristics of sealed-off stable CO_2 and CO lasers; long-term stabilization of CO_2 and CO lasers; precision heterodyne calibration; varactor photodiode detection; the determination of CO_2-isotope laser transitions; and CO_2 laser amplifiers.

Charles is a member of Tau Beta Pi, Eta Kappa Nu, and Sigma Xi. In 1979 he was elected a Fellow of the IEEE with the following citation: "For contribution to gas lasers and the pioneering development of ultrastable lasers."